MITOCHONDRIAL DNA REPLICATION IN SEA URCHIN OOCYTES

LLOYD MATSUMOTO, HARUMI KASAMATSU, LAJOS PIKÓ, and JEROME VINOGRAD

From the Developmental Biology Laboratory, Veterans Administration Hospital, Sepulveda, California 91343 and the Divisions of Biology and Chemistry, California Institute of Technology, Pasadena, California 91109

ABSTRACT

Mitochondrial DNA (mtDNA) replicative intermediates from *Strongylocentrotus purpuratus* oocytes were isolated by ethidium bromide-CsCl density gradient centrifugation and examined by electron microscopy after formamide spreading. In some experiments, the mtDNA was radioactively labeled by exposing isolated oocytes to [^{3}H]thymidine. Oocyte mtDNA replication appears to follow the displacement loop model outlined in mouse L cells. There are differences in detail. The frequency of D-loop DNA is much lower in oocytes, suggesting that the relative holding time at the D-loop stage is shorter. Duplex synthesis on the displaced strand occurs early and with multiple initiations. The frequency of totally duplex replicative forms, or Cairns' forms, is the highest reported for mtDNA. The differences may be related to the fact that oocyte mtDNA replication occurs in the absence of cell division and need not be coordinated with a cell cycle. Molecules with expanded D loops banded in the intermediate region between the lower and upper bands in an ethidium bromide-CsCl gradient, supporting the notion that displacement replication proceeds on a closed circular template which is subject to nicking-closing cycles. In mature sea urchin eggs, replicative forms are absent and virtually all the mtDNA is stored as clean circular duplexes. Some novel structural variants of superhelical circular DNA (molecules with denaturation loops and double branch-migrated replicative forms) are reported.

Mitochondria are among the cellular constituents which accumulate during oogenesis and are stored in the egg. As a result, animal eggs are greatly enriched in mitochondrial DNA (mtDNA).[1] Oocyte and egg mtDNA has been well characterized as to amount, location, circularity, and physical-chemical properties in several animal groups: amphibians (2, 3, 5), echinoderms (13, 14), and echiurids (4). However, there is relatively little information available on mitochondrial biogenesis and mtDNA replication in growing oocytes. In

[1] *Abbreviations used in this paper:* Cairns' form, replicative intermediate in which both daughter segments are double stranded; D-loop DNA, mitochondrial DNA with a single-stranded displacement loop of approximately 3% genome size; Exp-D DNA, replicative intermediate with an expanded D loop which may be totally or partially single stranded; KTE, 0.55 M KCl, 0.01 M Tris-HCl, 0.001 M EDTA, pH 7.6; mtDNA, mitochondrial DNA; TE, 0.01 M Tris-HCl, 0.001 M EDTA, pH 7.6. The terminology adopted in this paper follows that of Robberson et al. (16).

vivo long-term labeling experiments in the sea urchin have demonstrated incorporation of [^{3}H]thymidine into oocyte mtDNA (11, 14). Fine structural studies of oogenesis in sea urchins (20) as well as determinations of cytochrome *c* oxidase activity in developing oocytes of *Urechis caupo* (12) indicate that mitochondria are synthesized continuously during oogenesis. The formation of new mitochondria in growing sea urchin oocytes occurs in the absence of nuclear DNA replication (7).

This paper presents a study of mtDNA replication in developing oocytes of the sea urchin *Strongylocentrotus purpuratus*. The mtDNA was isolated by buoyant density centrifugation in ethidium bromide-CsCl gradients and analyzed by electron microscopy after formamide spreading. The replicative intermediates of oocyte mtDNA can be arranged in a pattern similar to that found in mouse L cells (8, 9, 16) and various normal and tumor tissues (22, 23). The following variations were observed: the oocyte mtDNA contains D-loop DNA at a low frequency; duplex synthesis on the displaced strand occurs early and is initiated at multiple sites; and the frequency of Cairns' forms is the highest reported so far for mtDNA. Replicative intermediates with expanded D loops were recovered primarily in the closed circular form, a result previously found for L-cell mtDNA (15) and for simian virus 40 (SV40) DNA (17). These findings demonstrate that a nicking-closing cycle is active during the course of replication.

The mtDNA in mature unfertilized eggs from two species of sea urchins was exclusively in the form of clean circular duplexes. This form is therefore considered to be the stable physiological storage form of mtDNA in these eggs.

We also describe some novel structural variants of superhelical mtDNA that have been observed on specimen grids prepared with the formamide technique.

MATERIALS AND METHODS

Isolation of Mature Eggs

Mature unfertilized eggs of the sea urchins *S. purpuratus* and *Lytechinus pictus* were collected by KCl injection of the animals (19). The eggs were washed three times in sea water and three additional times in 0.55 M KCl to remove the jelly coats.

Isolation of Oocytes

Oocytes were isolated by a procedure similar to that described by Giudice et al. (6). Ovaries from six to ten *S. purpuratus* females were removed after KCl shedding of the mature eggs. After three washes in Millipore-filtered Instant Ocean sea water (Aquarium Systems, Inc., Eastlake, Ohio) and three additional washes in 0.55 M KCl, 0.01 M Tris-HCl, 0.001 M EDTA, pH 7.6 (KTE), the ovaries (10–12 g wet weight) were teased and dissected into small pieces and digested for about 15 min under constant stirring in about 40 ml of a Pronase solution (1 mg/ml, B grade, Calbiochem, San Diego, Calif.) in KTE at room temperature. The suspension (excluding large debris) was washed three times with 200-ml ice-cold KTE by centrifugation at about 100 *g* for 10–15 s in a Sorvall HB-4 rotor (DuPont Co., Instrument Products Div., Newtown, Conn.). The final pellet was resuspended in 20 ml of KTE which was divided into four batches of 5 ml each, and each batch was layered on 40 ml of an isotonic linear sucrose gradient (0.15–0.85 M) constructed in the following manner: 1.5 parts 1 M sucrose in 0.01 M Tris-HCl, 0.001 M EDTA, pH 7.6 (TE buffer) was diluted with 8.5 parts KTE to obtain an isotonic 0.15 M sucrose solution, and 8.5 parts 1 M sucrose in TE was diluted with 1.5 parts KTE to give an isotonic 0.85 M sucrose solution; these two solutions were then used to form an isotonic linear sucrose gradient. After centrifugation for 1–1.5 min at about 100 *g* in a Sorvall HB-4 rotor, the suspension was separated into the following main components: ovarian tissue cells in the upper portion of the gradient; mature eggs, large oocytes, and debris near the bottom of the tube; and an enriched band of small to medium oocytes in the middle of the gradient. The oocytes were collected by pipette, washed twice with KTE, resuspended in 10 ml KTE, and recentrifuged on the isotonic 0.15–0.85 M sucrose gradient as above. The oocytes were washed twice in KTE (for the isolation of mitochondria) or in sea water (for incubation with [^{3}H]thymidine). The yield of oocytes was about 2–6% of the wet weight of the ovaries used. The yield was higher early in the reproductive season.

Isotope Labeling

Isolated oocytes were incubated in 10 vol of sea water containing 200 μCi/ml [*methyl*-^{3}H]thymidine (52.7 mCi/μmol, New England Nuclear, Boston, Mass.). The oocytes were washed six times (50 ml/wash) with ice-cold KTE after 4 h of incubation with gentle shaking at 16°–18°C.

Isolation of Mitochondria

Mature unfertilized eggs or oocytes (either isolated freshly or after incubation with [^{3}H]thymidine) were suspended in eightfold volume of ice-cold 0.4 M sucrose in TE and were homogenized with 10 strokes in a Potter-Elvehjem homogenizer (Arthur H. Thomas Co., Philadelphia, Pa.). The molarity of the homogenate was adjusted to 1 M sucrose with 2 M sucrose in TE. After dilution with 1 M sucrose in TE as needed, the homoge-

nate was layered on 3 ml of 1.5 M sucrose and centrifuged in an SW25.1 rotor at 23 krpm for 30 min at 5°C in a Beckman L2-65B ultracentrifuge (Beckman Instruments, Inc., Spinco Div., Palo Alto, Calif.). Dense cellular constituents pelleted at the bottom of the tube, mitochondria migrated to the 1.0–1.5 M sucrose interface, and yolk formed a cap at the top of the gradient. The mitochondria were collected by pipette and washed once with KTE.

Isolation of mtDNA

The final mitochondrial pellet was suspended in 1 ml of 0.5 M NaCl, 0.1 M Tris-HCl, 0.01 M EDTA, pH 8.0, and lysed with an equal volume of prewarmed (37°C) 4% dodecyl sodium sulfate (M C & B Manufacturing Chemists, Cincinnati, Ohio) in distilled water. A sample of ^{14}C-labeled SV40 marker DNA containing components I and II was added at this point. The lysate was adjusted to a final density of 1.55 g/ml with CsCl (optical grade, Harshaw Chemical Co., Solon, Ohio) and to about 400 μg/ml ethidium bromide (Boots Pure Drug Co., Ltd., Nottingham, England) in a total volume of 3.5 ml in a 5-ml polyallomer tube. After centrifugation for 18 h at 40 krpm, 20°C, in the Beckman SW50.1 rotor the contents of the tube (except for the pellet and top layer) were transferred to a second tube and centrifuged for 44 h at 38 krpm. In the experiments with labeled oocytes, the gradients were fractionated in 40-μl fractions and an aliquot of each fraction was assayed for radioactivity in a Beckman LS-200 scintillation counter. The Whatman 3 MM discs were air dried, washed in three changes of cold 5% TCA, and dehydrated in ethanol and ether for counting. The remainder of the fractions was used for analyses by electron microscopy. In the experiments with unlabeled oocytes, all of the mtDNA from the region spanning the upper and lower bands in the gradient was collected and prepared for electron microscopy. In the study of mtDNA from mature unfertilized eggs, the lower band DNA (containing the major portion of the total DNA) was collected from the EthBr-CsCl gradient; this DNA was prepared for electron microscopy either directly or after a further purification step by band velocity sedimentation in EthBr-CsCl (9).

Electron Microscopy

Fractions collected from the EthBr-CsCl gradient were dialyzed in the dark at 4°C against several changes of 0.1 M NaCl, 0.1 M Tris, 0.01 M EDTA, pH 8.5, containing Dowex 50WX8 resin (Bio-Rad Laboratories, Richmond, Calif.). The DNA was concentrated in the dialysis tubing with dry Sephadex 200 (Pharmacia, Uppsala, Sweden) and dialyzed again. Formamide spreading of the DNA was carried out as described (9) except that the formamide concentration in the hypophase was 17% instead of 10% and the final cytochrome *c* concentration was 40 μg/ml. Films were picked up on parlodion-coated 300-mesh copper grids, rotary shadowed with Pt-Pd, and examined in a Philips EM200 or 300 at an accelerating voltage of 40 or 60 kV. Photographs were taken at a magnification of about × 5,000. The lengths of the single- and double-stranded regions in the molecules were measured from tracings of negatives enlarged on a Nikon 6F projection comparator. For an analysis of duplex synthesis on the displaced strand (Figs. 3 and 4), randomly selected squares on the grid were scanned and all Exp-D molecules (except for those having extensive entangled regions) were photographed; molecules containing D loops (less than 5% of genome size) were generally excluded from this sample. In these preparations the contour lengths of single-stranded ϕX DNA and duplex RF ϕX DNA, which were used as internal standards, were equal.

RESULTS

Isolated Oocytes

The isolated oocytes and the purity of the preparations used in these studies are illustrated in Fig. 1. The mean oocyte diameter of 186 randomly measured oocytes was 41 ± 9 μm SD, with a size range of 20–76 μm. The bulk of the oocytes was of medium size, 30–60 μm, and was in the vitellogenesis stage (20). Mature *S. purpuratus* oocytes are about 80 μm in diameter (18).

Replicative Forms in Total Oocyte MtDNA

The types and frequencies of the various replicative forms in the total mtDNA from *S. purpuratus* oocytes are shown in Table I. Contamination with linear DNA amounted to about 10% in these samples. In two such preparations, the replicative forms accounted for 21 and 14% of the circles. Molecules with D loops were relatively infrequent, 7 and 4%, and constituted about 30% of replicative forms; the average size of the D loop in 17 molecules was 3.2 ± 0.7% of the genome size. Gapped circular molecules (Fig. 2 *e*) were scarce. Molecules with expanded D loops represented by far the most frequent class and were used for an analysis of the occurrence and the initiation of duplex synthesis.

Duplex Synthesis in Exp-D Molecules

Electron microscope examination revealed that duplex synthesis had occurred in 90% of Exp-D molecules. Cairns' forms, i.e., totally double-stranded replicating intermediates, were frequent and accounted for 25% of the Exp-D molecules, and molecules with partial duplex synthesis accounted for 65%. Fig. 2 illustrates the various types of replicating intermediates and Fig. 3

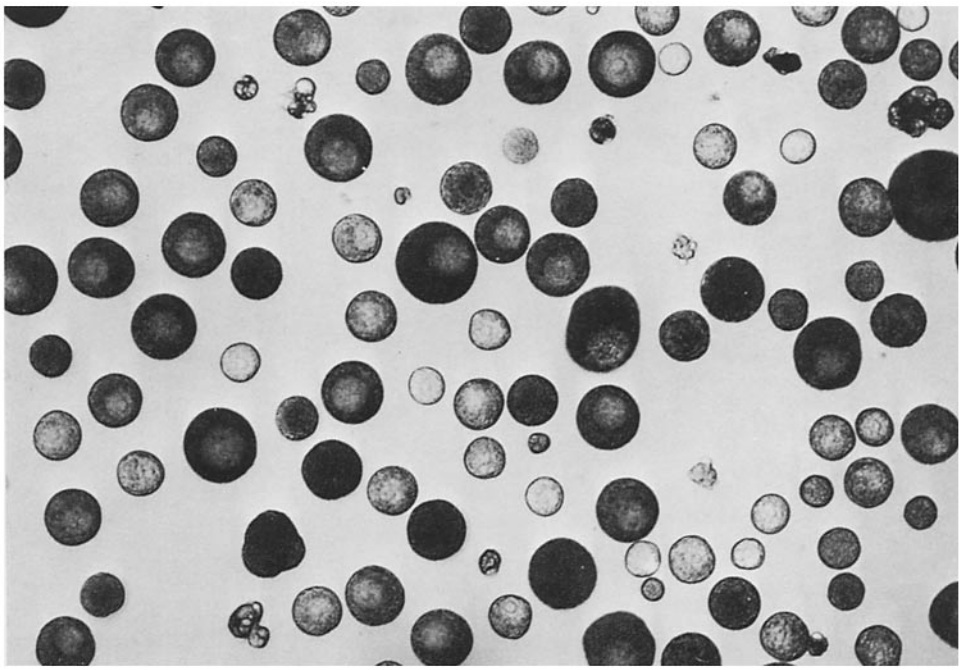

FIGURE 1 Photomicrograph of isolated *S. purpuratus* oocytes. Larger oocytes are darker due to the accumulation of yolk and pigment granules. The germinal vesicle can be seen as a light area in the cytoplasm. × 160.

TABLE I

Distribution of Replicative Forms in Total MtDNA from S. purpuratus Oocytes

Duplex circles	Preparation	
	a	*b*
	%	%
Clean	79	86
With D loops	7	4
With Exp-D loops*	13	9
With gaps	1	1
Total molecules	159	172

* About 20% of Exp-D molecules exhibited branch migration (see below) and are included in this class.

presents the data from which the above percentages were derived.

Fig. 3 shows the relative size of the duplex region(s), in the expanded segment of 79 Exp-D molecules and nine D-loop molecules from preparation *a* of Table I as a function of expansion. Duplex synthesis has occurred in all molecules that have expanded through 0.15–0.20 genome size, except for one molecule with a fully single-stranded expansion of 0.34 genome size. In molecules with larger expansions, the amount of duplex synthesis is in general linearly related to the degree of expansion. A total of 22 molecules was Cairns' forms, with expansions varying from D-loop size to 0.8 genome size.

Fig. 4 diagrammatically illustrates the distribution of duplex regions in 50 expansions from the above population of molecules (Cairns' forms and totally single-stranded expansions have been omitted). Multiple duplex segments are present in 22 expansions with up to five such segments in a single expansion. At least one fork contained a single-stranded region in all Exp-D molecules other than the Cairns' forms. Several alternative orientations of the expansions in Fig. 4 were examined, but no clearcut pattern emerged to indicate that initiation of the duplex segments occurred at unique sites on the displaced strand.

Distribution of Replicative Forms of MtDNA in EthBr-CsCl Gradients

Fig. 5 shows the EthBr-CsCl buoyant density gradient profile of ^{3}H-labeled mtDNA from *S.*

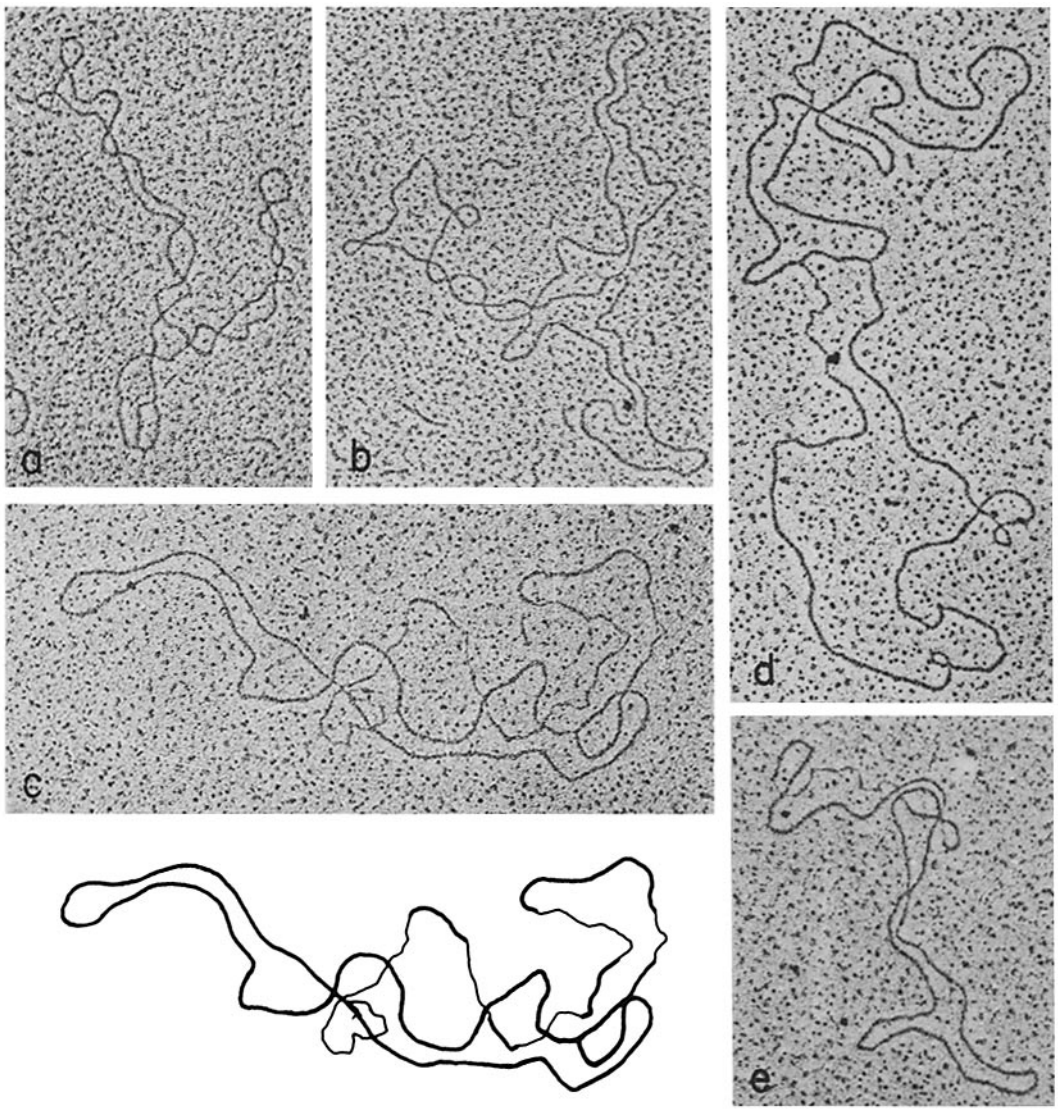

FIGURE 2 Electron micrographs of replicative forms of oocyte mtDNA. Fig. 2 *a*, Cairns' form with a D-loop size expansion. Fig. 2 *b*, Cairns' form with a 0.5 genome size expansion. Fig. 2 *c*, Exp-D molecule with a 0.7 genome size expansion containing multiple double-stranded segments; the thick and thin lines in the corresponding drawing represent duplex and single-stranded regions, respectively. Fig. 2 *d*, Exp-D molecule with a nearly complete expansion containing a large double-stranded segment and a small single-stranded segment at one of the forks. Fig. 2 *e*, gapped circle with a single-stranded segment of 0.11 genome size. The contour length of the genome is 5 μm. $\times$ 40,000.

purpuratus oocytes incubated with [^{3}H]thymidine for 4 h. Components I and II of ^{14}C-labeled SV40 DNA serve as markers. The ^{3}H radioactivity is distributed throughout the gradient between the lower and upper bands, with the amount of label increasing more or less uniformly toward the upper band. The intermediate region between the two bands is heavily labeled. Some of the radioactivity in the upper band could have derived from nuclear DNA contamination from ovarian accessory cells. A small amount of label is banded at a dense region of the gradient (Fig. 5, fraction *A*) and is

presumably associated with sea urchin egg polysaccharide (13); electron microscope examination failed to reveal DNA in this band.

The frequencies of various forms of mtDNA in different regions of the gradient (Fig. 5, fractions *B–G*) were determined by electron microscopy and are shown in Table II. Samples from the intermediate region of the gradient (Fig. 5, fractions *D*, *E*) were greatly enriched in mtDNA molecules with expanded D loops, a high proportion of which (about 80%) was totally duplex or Cairns' forms. A substantial portion of these molecules exhibited double-branch migration (Fig. 9) and several Exp-D molecules contained single-stranded denaturation loop(s) (Fig. 7 *b*); these forms are discussed below. Gapped circular molecules were present only in the upper band region (Fig. 5, fractions *F*, *G*); most of the gaps were on the order of 1–3% genome size. D-loop molecules were observed infrequently in the lower and intermediate regions of the gradient. The reason for the scarcity of D-loop DNA is not clear but it could have been due to the occurrence of D-loop expansion in the absence of D-loop initiation in the isolated oocytes. Nicking in the system appeared to be low and the bulk of the mtDNA sedimented in the lower band as observed by fluorescence in the gradient when viewed with ultraviolet light.

MtDNA of Mature Eggs

Table III shows the results of an electron microscope study of mtDNA from mature, unfertilized eggs of two sea urchin species. Virtually all the DNA in these eggs was found as clean circular duplexes (Fig. 6).

We measured the size of the mtDNA from *S. purpuratus* and *L. pictus* eggs with respect to double-stranded RF ϕX174 DNA. Two adjacent ϕX DNA molecules were measured for each mtDNA molecule. The ratios of contour lengths of mtDNA and ϕX DNA were 2.89 ± 0.07 SD for *S. purpuratus* (n = 47) and 2.91 ± 0.09 SD for *L. pictus* (n = 44). This gives a mean molecular weight of 10.0×10^6 daltons for sea urchin mtDNA, if the molecular weight of RF ϕX174 DNA is taken as 3.45×10^6 daltons (10). The corresponding B-form length of sea urchin mtDNA, 5.1 μm, is somewhat larger than the values obtained earlier for *L. pictus* mtDNA,

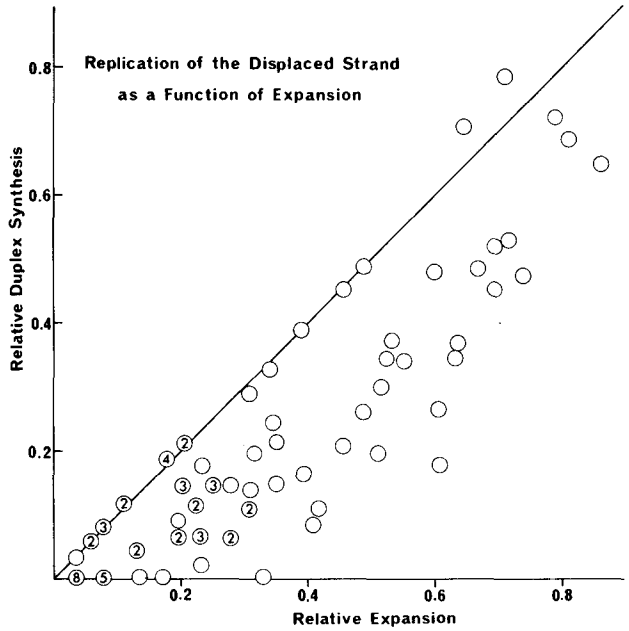

FIGURE 3 Relative duplex synthesis on the displaced strand in Exp-D molecules from a mtDNA preparation from *S. purpuratus* oocytes. The length of the duplex segment(s) on the displaced strand is plotted as a function of the expansion; the units are in genome size. The numbers within the symbols indicate the number of overlapping data points. The diagonal line gives the position for fully double-stranded expansions or Cairns' forms.

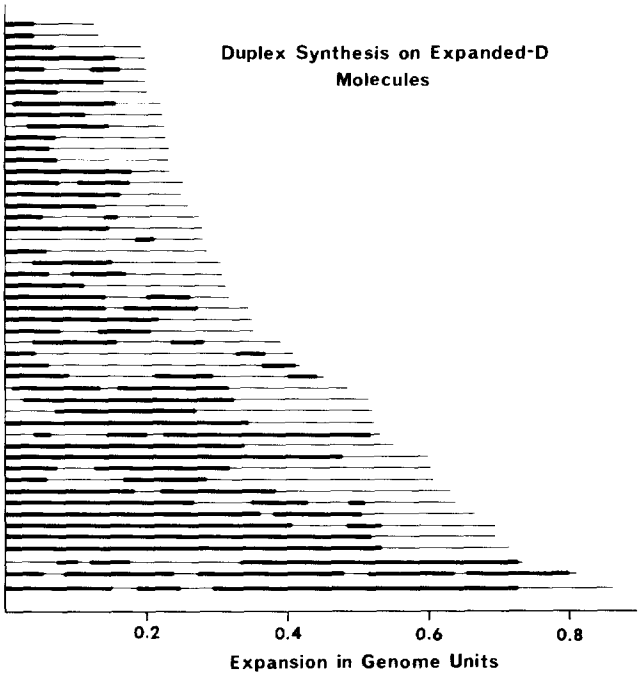

FIGURE 4 Diagram of displaced strands from 50 Exp-D molecules showing distribution of duplex segments. The molecules were derived from the same population of molecules shown in Fig. 3 but Cairns' forms and totally single-stranded loops have been omitted. Expansions with a duplex segment at one fork are oriented so that the duplex segment is at 0 expansion; expansions with single-stranded segments at both ends are randomly oriented. The thick and thin lines represent duplex and single-stranded regions, respectively.

4.45–4.85 μm, on the basis of electron microscope calibration methods (13, 14).

Structural Variants of Superhelical MtDNA

MOLECULES WITH DENATURED REGIONS: In the course of this work several unreported DNA structures were observed. Simple closed circular mitochondrial and SV40 DNA molecules with single-stranded denaturation loops (Fig. 7 *a*) were seen at frequencies of about 2 and 5%, respectively, in the DNA from the lower band of an EthBr-CsCl gradient (Fig. 5, fractions *B–D*). These DNAs are regarded as closed molecules because of their buoyant positions. They were absent in the open circular DNA sample from the upper band (Fig. 5, fractions *F*, *G*). The denatured region accounted for 2 and 4% of the contour length in the mitochondrial and SV40 DNA. A study of the occurrence of such molecules in preparations of SV40, PM2, and mitochondrial DNA, to be reported elsewhere, has indicated that these denaturation loops arise as a result of the "early melting" (21) of superhelical DNAs having negative superhelical turns. The removal of the superhelical turns results in a relaxed circular conformation and the formation of a denatured (unwound) duplex region localized in a presumed A-T-rich region. These molecules have previously escaped detection because, in part, they were unexpected and also possibly because of minor variations in the technique of specimen preparation. For example, these structures are not observed if the salt concentration in the DNA-cytochrome solution is elevated over that used in this work as described in Materials and Methods.

Denaturation loop(s) were also observed in closed replicative intermediates isolated from an intermediate region between the lower and upper bands in an EthBr-CsCl gradient (Fig. 5, fraction *E*). As in the example shown in Fig. 7 *b*, the denaturation loop always occurs in the nonreplicated region which we assume was originally negatively supercoiled and melted as described. The duplex in the replicated region contains a

minimum of two swivels, one at each fork, and, therefore, is not subject to the thermodynamic instability referred to above as causing the early melting of negatively superhelical DNA.

REPLICATIVE INTERMEDIATES WITH LINEAR DUPLEX SEGMENT(S) EMERGING FROM THE FORK(S): Several complex structures were observed on specimen grids prepared with fractions *C–F*, Fig. 5 (see Table II). Among the larger replicative intermediates in these fractions, 20% were interpretable as double branch-migrated (1, 10) closed Exp-D molecules illustrated diagrammatically in Fig. 8 B. These molecules all contained denaturation loops in the nonreplicated region. Electron micrographs of three such molecules are shown in Fig. 9. In the first two (Fig. 9 *a* and *b*), the junction of the four duplexes at each of the replicating forks is clearly visible as a small,

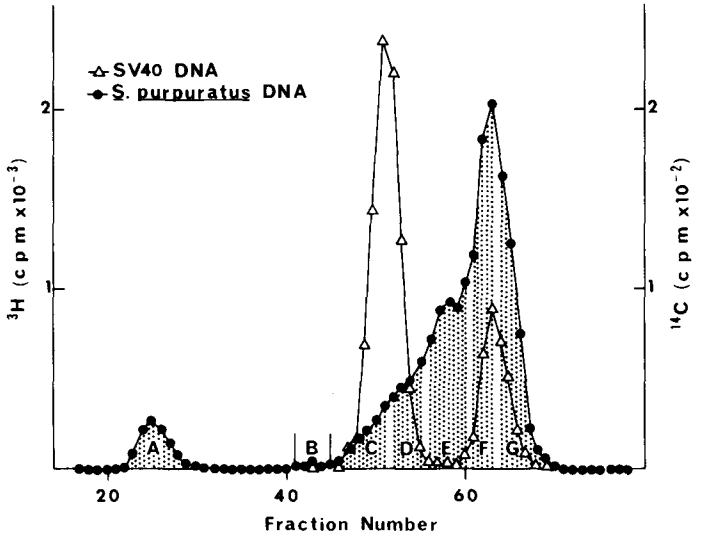

FIGURE 5 Ethidium bromide-CsCl buoyant density gradient profile of ^{3}H-labeled DNA extracted from the mitochondrial fraction of *S. purpuratus* oocytes incubated with [^{3}H]thymidine for 4 h. The gradient also contained a sample of ^{14}C-labeled SV40 marker DNA. For procedures see Materials and Methods. Fractions in the stippled areas (designated by capital letters) were pooled and used for electron microscopy (see Table II).

TABLE II

Distribution of Replicative Forms of Oocyte MtDNA in EthBr-CsCl Gradient

Duplex circles*	Fraction‡					
	B	C	D	E	F	G
	%	%	%	%	%	%
Clean	99	99	81	55	85	87
With D loops	1		2	1	1	
With Exp-D loops						
Duplex (Cairns')			12	21	4	3
Containing single strands			2	8	3	3
Branch migrated		1	2	12	1	
With denatured regions				3		
With gaps					6	7
Total molecules	93	119	123	108	98	70

* Catenated molecules are not scored.

‡ Fractions from the gradient shown in Fig. 5.

almost rectangular, single-stranded loop. In the third example (Fig. 9 *c*), no junction loops are visible. The size of the junction loop is variable but on the average corresponds to about 100 nucleotides and could have resulted from the symmetric melting of 12 base pairs in each of the four duplexes forming the junction region as illustrated diagrammatically in Fig. 8 C. The linear duplex segments with free ends that emerge from the replicating forks (Fig. 8 B) were usually of unequal length. In one molecule out of 17, one of the emerging linears was entirely single stranded; in the others the emerging linear segments were entirely duplex.

We propose that the emerging duplex segments have arisen by double-strand branch migration as shown diagrammatically in Fig. 8 A and B. The complementary progeny strands form an emerging linear duplex segment at each fork while the corresponding parental strands base pair to form a duplex within the closed circle. This process requires the introduction of negative superhelical turns or denaturation loops to maintain the topological winding number constant. Alternatively, if a denaturation loop is formed in the structure shown in Fig. 8 A, branch migration would occur (in the absence of supercoiling) to conserve the topological winding number (21). The observed molecules (Fig. 9) contain some crossovers and two to four denatured single-stranded looped regions. The loops are always in the nonreplicated region and are not seen in the nonconstrained replicated regions. If the total length of the emerging linear duplex segments is taken to be a

TABLE III

Frequencies of Replicative Forms of MtDNA in Unfertilized Sea Urchin Eggs

Number of duplex circles	*S. purpuratus**	*L. pictus*‡
Clean	1,727	830
With D loop	1	0
With expanded D loop	1	0
With single-stranded tail	1	0
With double-stranded tail	1	1
Total molecules	1,731	831

* Pooled data from four preparations.

‡ Pooled data from two preparations.

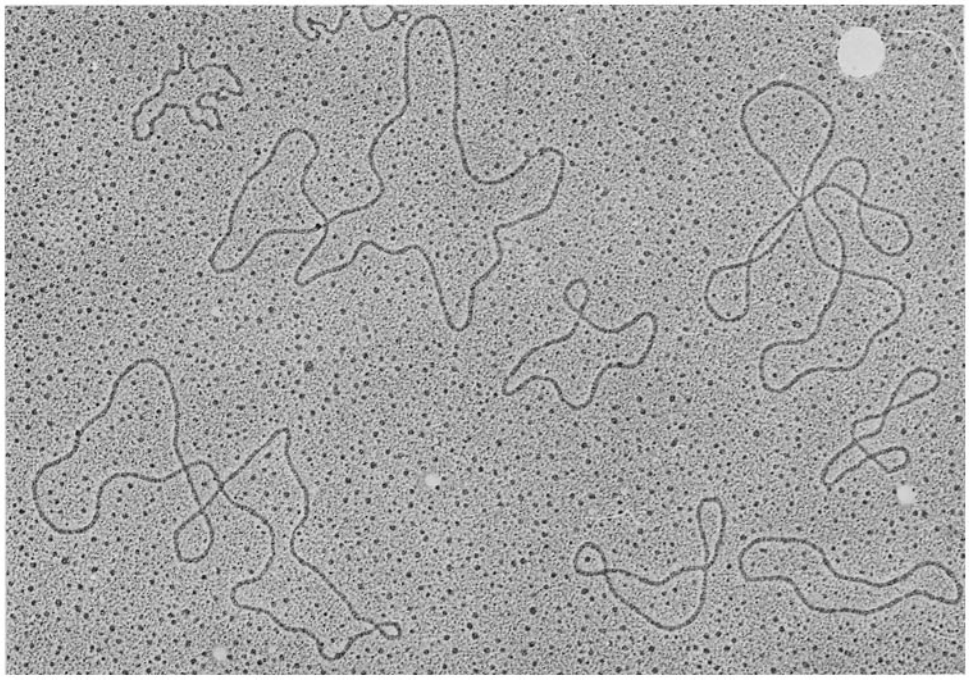

FIGURE 6 Electron micrograph showing clean circles of mtDNA from mature, unfertilized eggs of *S. purpuratus*. The DNA was prepared for electron microscopy by the formamide technique. The small circles are RF ϕX174 DNA. × 40,000.

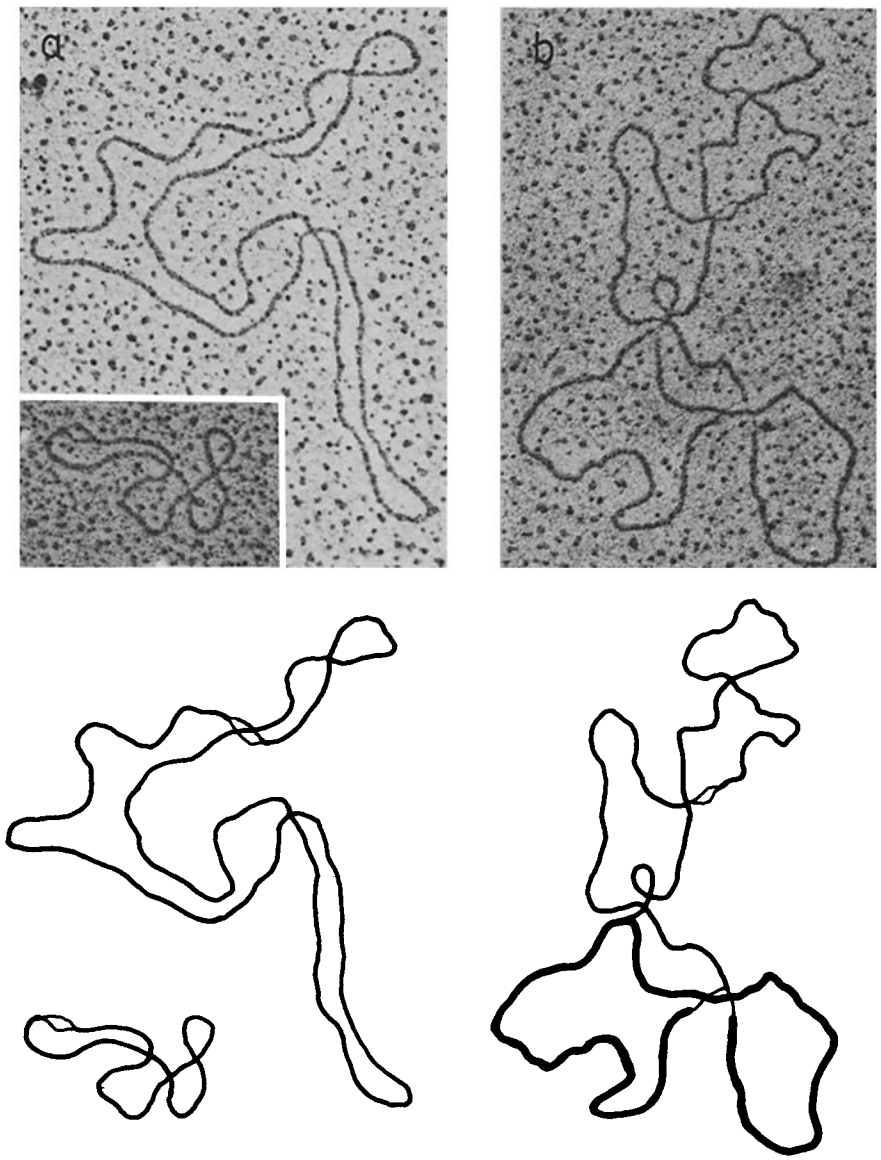

FIGURE 7 Electron micrographs of oocyte mtDNA molecules with denaturation loops. Fig. 7 *a*, a mtDNA circle with a denaturation loop; *inset*, a SV40 DNA circle with a denaturation loop. Fig. 7 *b*, a Cairns' form with a denaturation loop and a denatured region at one of the forks. × 60,000. In the corresponding line drawings the thin line represents single strands, the medium-heavy line represents double-stranded portions of the parent molecule, and the extra-heavy line represents double-stranded daughter segments.

measure of the extent of duplex formation within the closed circle, we would expect that the total length would be equal to one-half the sum of the contour lengths of the denaturation loops in the nonreplicated region. Actually, six of the 17 molecules are in accord with the relation as shown in Fig. 10. In the remainder, the contour lengths of the denaturation loops are shorter by as much as 50% than expected. This could have resulted from the formation of a number of smaller loops which were too small to be detected or, alternatively, from a failure of some of the denaturation loops to

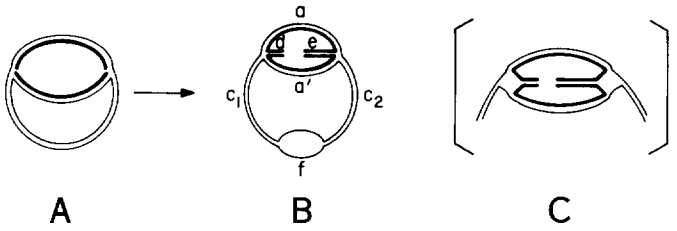

FIGURE 8 Schematic diagrams illustrating branch migration in covalently closed replicative intermediates. Thick and thin lines represent progeny strands and parental strands, respectively. Fig. 8 A, Cairns' type replicative intermediate. In Fig. 8 B, *d* and *e* represent the lengths of the branch-migrated linear duplex segments; *a* and *a'*, the replicated regions remaining after branch migration; c_1 and c_2, duplex segments in the nonreplicated region; and *f*, the length of the denatured loop. Fig. 8 C illustrates the partial melting at the fork regions.

spread out fully on the electron microscope specimen grid.

The molecules which have undergone branch migration are clearly replicative intermediates because, as indicated in Fig. 8 B, the lengths *a* and *a'* were equal to each other and the sum $((a' + a)/2, c_1, c_2,$ and $f/2)$ was equal to the monomer length. The extent of replication, $((a + a')/2 + d + e)$ 100/(monomer length), varied from 16 to 68% among the 17 molecules analyzed as shown in the inset in Fig. 10. It may be calculated from the inset that approximately one-third of the replicated regions in these molecules had branch migrated.

At the present time the driving force for the double-branch migration or, alternatively, for the formation of the denaturation loops is not understood, nor can we account for the fact that only one-fifth of the large replicating forms underwent branch migration.

DISCUSSION

Because of the large number of mitochondria in sea urchin oocytes, we have been able to obtain relatively clean preparations of mtDNA with simple preparative procedures and without DNase treatment of the mitochondria. Our results show that the replicative intermediates of oocyte mtDNA are similar to those found in mouse L cells (8, 9, 16) and in rat liver and rat hepatoma cells (22, 23). However, there are several differences as outlined below.

The frequency of D-loop molecules in total oocyte mtDNA, 4–7%, is the lowest reported so far. A substantial loss of D loops is considered to be unlikely because of the apparent low rate of nicking during isolation. The low frequency of D-loop molecules suggests that the relative duration of this holding stage in mtDNA replication is shorter in these cells. Another difference from the model derived from the study of mtDNA replication in L cells is in the pattern of duplex synthesis on the displaced strand. In sea urchin mtDNA duplex synthesis is initiated in nearly all molecules with an expansion of 15–20% as against approximately 60% expansion in L cells (16). During further expansion, the rate of duplex synthesis keeps pace with the rate of expansion (Fig. 3). About 25% of expansions contain multiple duplex segments (Fig. 4), indicating that duplex synthesis takes place with multiple initiations. Cairns' forms, varying in size from D-loop to 0.8 genome size, are frequent: about 25% of Exp-D molecules in a total mtDNA preparation from freshly isolated oocytes and about 80% of larger replicative intermediates in a preparation obtained from cultured oocytes. The frequency of Cairns' forms is considerably higher than that observed in other systems, namely, about 1% of Exp-D molecules of mtDNA in L cells (16) and 3–8% of all double-forked molecules in normal rat liver and rat hepatoma cells (23). It is clear that the degree to which displacement and duplex syntheses are synchronized may vary in different systems, for reasons which are not understood at present. The low frequency of gapped circles in the oocyte DNA is consistent with the high frequency of Cairns' forms. The gapped circles have been postulated to arise upon separation of fully expanded replicating intermediates before duplex synthesis has been completed (16).

The results of isotope labeling experiments (Fig. 5) show that isolated oocytes take up and incorporate [^{3}H]thymidine into mtDNA. The observation that Exp-D molecules are located primarily in the intermediate region of an EthBr-CsCl gradient

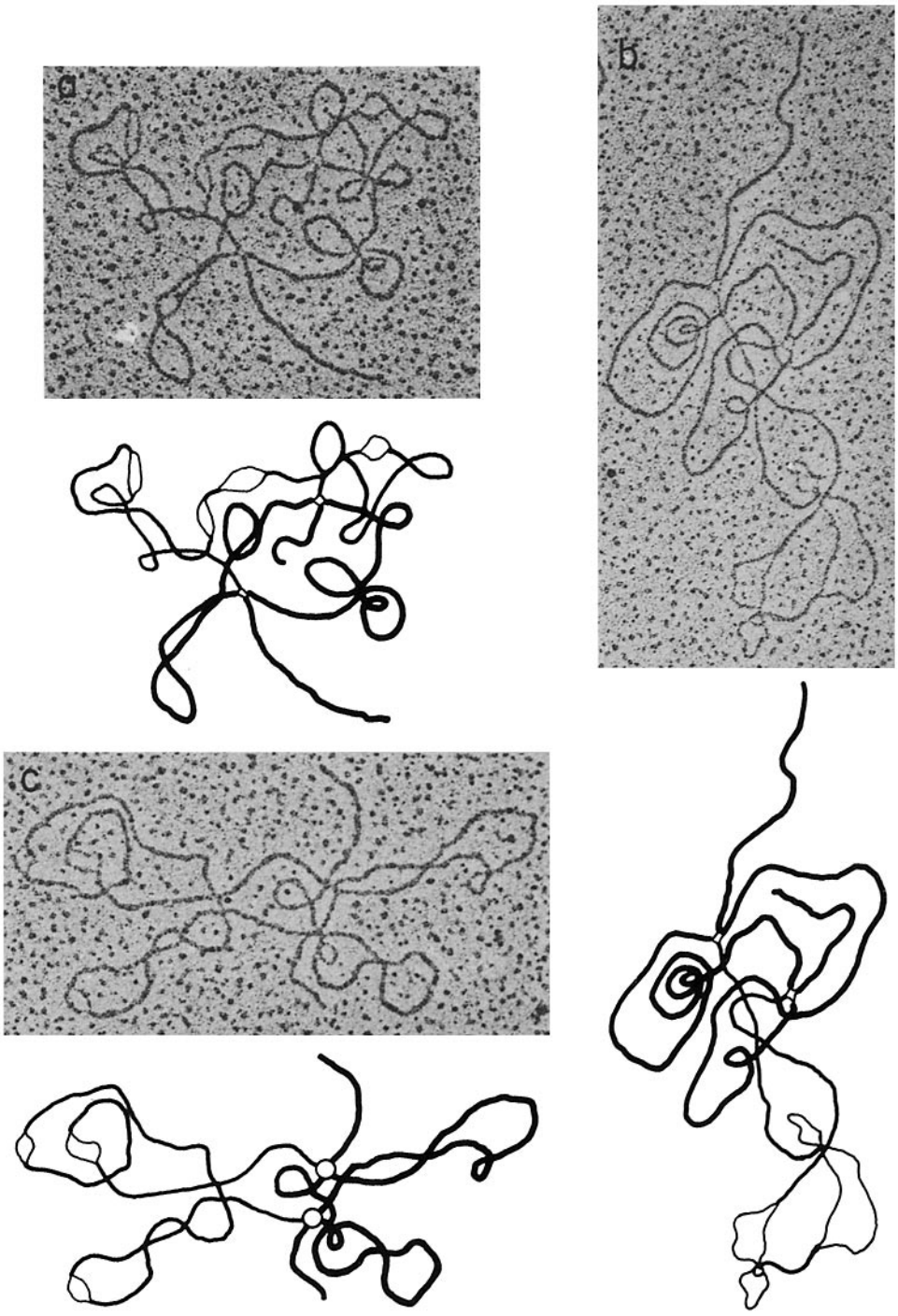

FIGURE 9 Electron micrographs of branch-migrated replicating intermediates of oocyte mtDNA. In the corresponding line drawings, the replicated regions and the branch-migrated linear progeny duplex segments are represented by extra-heavy lines. Duplex and denatured segments in nonreplicated regions are represented by thick and thin lines, respectively. The small circles in the line drawing for Fig. 9 *c* indicate the junction sites at which the branch-migrated progeny linear duplexes meet the replicated and nonreplicated duplex segments of the parent molecule. × 50,000.

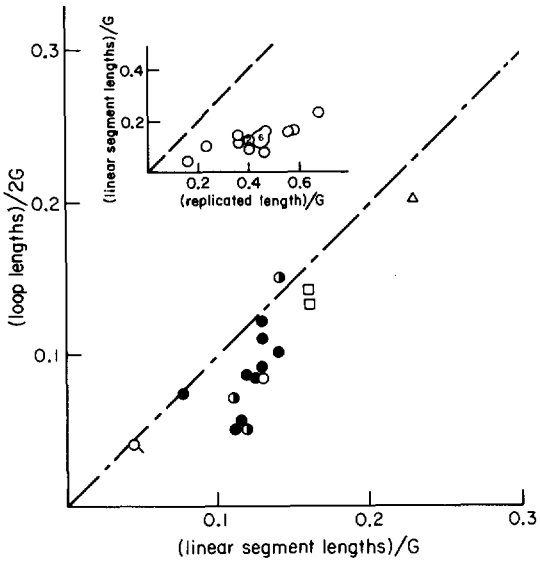

FIGURE 10 The length of the linear segments as a function of the lengths of visible denatured loops and the extent of replication. The lengths in each of 17 branch-migrated replicating intermediates were measured (see Fig. 8 B) and normalized to a monomer genome length (G). In the large diagram, the fractional length of the sum of the denaturation loops (loop lengths/2G) is plotted as a function of the fractional length of the sum of branch-migrated linear segments (linear lengths/G). Symbols in the graph represent the extent of replication expressed as a fractional genome size calculated with the relation $((a + a')/2 + d + e)$/(monomer length); (Q) 0.1–0.2 G; (○) 0.2–0.3 G; (◑) 0.3–0.4 G; (●) 0.4–0.5 G; (□) 0.5–0.6 G; and (△) 0.6–0.7 G. *Inset*, the extent of double-branch migration plotted as a function of the extent of replication. The numbers in the symbols indicate the overlapped data points.

(Fig. 5 and Table II) indicates that these molecules are covalently closed as has been shown for replicating mtDNA in L cells (15) and for SV40 DNA (17). These findings imply that displacement synthesis is accompanied by nicking-closing cycles.

The duration of a complete cycle of replication of mtDNA in *S. purpuratus* oocytes is difficult to estimate since the time needed for the completion of oocyte growth is not known. However, on the basis of studies of oogenesis in wild *S. purpuratus* females (7), the duration of oocyte growth from 20 to 80 μm (mature) size can be roughly estimated at 3–4 wk, giving a doubling time for oocyte volume of about 4 days. Since about 10–14% of mtDNA in a total oocyte preparation (Table I) are replicating forms (exclusive of D-loop molecules), the replication time of a mtDNA molecule can be estimated at about 10–14 h. The corresponding overall rate of replication (about 0.007 μm/min) is similar to that estimated for rat liver mtDNA (23) but is considerably slower than the 0.1 μm/min calculated for mtDNA in L cells (16).

At the termination of oogenesis, sea urchin eggs undergo nuclear maturation and are stored in the ovary until spawning and fertilization. Nearly all the mtDNA recovered from maure, unfertilized eggs of *S. purpuratus* and *L. pictus* were present in the form of covalently closed, clean circular duplexes. A loss of D loops during isolation of the mtDNA is considered highly unlikely, since special care was taken in the preparative procedures and spreading for electron microscopy was carried out as expeditiously as possible, without any intervening storage of the DNA. We conclude that mtDNA in these eggs is stored as clean duplex circles. Electron microscope analyses of mtDNA from sea urchin embryos indicate that the mtDNA remains in this form throughout early development at least until the early pluteus stage (Matsumoto and Pikó, unpublished observations). However, this observation is not generally true for animal eggs, since over 80% of mtDNA molecules in unfertilized frog eggs contain D loops (Hallberg, personal communication). The reason for this difference is unknown but it may be related to differences in the state of nuclear and cytoplasmic maturation in these eggs. The sea urchin egg is fertilized after nuclear maturation has been completed whereas in vertebrate eggs fertilization takes place at the second maturation metaphase.

We thank Ms. Phyllis Hotchkin and Ms. Roxanne Meyer for technical assistance.

This work was supported in part by United States Public Health Service, National Institutes of Health grants CA08014 from the National Cancer Institute and GM15327 from the National Institute of General Medical Sciences. L. Matsumoto was supported by National Institutes of Health postdoctoral fellowship 1 FO-CA53287-01 from the National Cancer Institute and H. Kasamatsu was the recipient of a postdoctoral fellowship from the Helen Hay Whitney Foundation.

This is contribution no. 4845 from the Division of Chemistry and Chemical Engineering, California Institute of Technology.

Received for publication 1 March 1974, and in revised form 3 May 1974.

Note added in proof: R. L. Hallberg has recently published (*Dev. Biol.* **38**:346–355) his data showing a high percentage of D loops (at least 76%) in total mtDNA from unfertilized eggs of *Xenopus laevis;* he also ob-

served D loops in the mtDNA from unfertilized eggs of three other amphibian species. Recently we have found 30% D-loop DNA in total mtDNA from unfertilized mouse eggs (Matsumoto and Pikó, unpublished).

REFERENCES

1. BROKER, T. R., and I. R. LEHMAN. 1971. Branched DNA molecules: intermediates in T4 recombination. *J. Mol. Biol.* **60**:131–149.
2. DAWID, I. B. 1965. Deoxyribonucleic acid in amphibian eggs. *J. Mol. Biol.* **12**:581–599.
3. DAWID, I. B. 1966. Evidence for the mitochondrial origin of frog egg cytoplasmic DNA. *Proc. Natl. Acad. Sci. U. S. A.* **56**:269–276.
4. DAWID, I. B., and D. D. BROWN. 1970. The mitochondrial and ribosomal DNA components of oocytes of *Urechis caupo*. *Dev. Biol.* **22**:1–14.
5. DAWID, I. B., and D. R. WOLSTENHOLME. 1967. Ultracentrifuge and electron microscope studies on the structure of mitochondrial DNA. *J. Mol. Biol.* **28**:233–245.
6. GIUDICE, G., G. SCONZO, A. BONO, and I. ALBANESE. 1972. Studies on sea urchin oocytes. I. Purification and cell fractionation. *Exp. Cell Res.* **72**:90–94.
7. HOLLAND, N. D., and A. C. GIESE. 1965. An autoradiographic investigation of the gonads of the purple sea urchin (*Strongylocentrotus purpuratus*). *Biol. Bull.* (*Woods Hole*). **128**:241–258.
8. KASAMATSU, H., L. I. GROSSMAN, D. L. ROBBERSON, R. WATSON, and J. VINOGRAD. 1973. The replication and structure of mitochondrial DNA in animal cells. *Cold Spring Harbor Symp. Quant. Biol.* **38**:281–288.
9. KASAMATSU, H., D. L. ROBBERSON, and J. VINOGRAD. 1971. A novel closed-circular mitochondrial DNA with properties of a replicating intermediate. *Proc. Natl. Acad. Sci. U.S.A.* **68**:2252–2257.
10. KIM, J.-S., P. A. SHARP, and N. DAVIDSON. 1972. Electron microscope studies of heteroduplex DNA from a deletion mutant of bacteriophage ϕX-174. *Proc. Natl. Acad. Sci. U. S. A.* **69**:1948–1952.
11. MATSUMOTO, L., and L. PIKÓ. 1971. *In vivo* radioactive labeling of mitochondrial DNA in *Arbacia punctulata* oocytes. *Biol. Bull.* (*Woods Hole*). **141**:397. (Abstr.).
12. MILLER, J. H., and D. EPEL. 1973. Studies of oogenesis in *Urechis caupo*. II. Accumulation during oogenesis of carbohydrate, RNA, microtubule protein, and soluble, mitochondrial, and lysosomal enzymes. *Dev. Biol.* **32**:331–344.
13. PIKÓ, L., D. G. BLAIR, A. TYLER, and J. VINOGRAD. 1968. Cytoplasmic DNA in the unfertilized sea urchin egg: physical properties of circular mitochondrial DNA and the occurrence of catenated forms. *Proc. Natl. Acad. Sci. U. S. A.* **59**:838–845.
14. PIKÓ, L., A. TYLER, and J. VINOGRAD. 1967. Amount, location, priming capacity, circularity and other properties of cytoplasmic DNA in sea urchin eggs. *Biol. Bull.* (*Woods Hole*). **132**:68–90.
15. ROBBERSON, D. L., and D. A. CLAYTON. 1972. Replication of mitochondrial DNA in mouse L cells and their thymidine kinase$^-$ derivatives: displacement replication on a covalently-closed circular template. *Proc. Natl. Acad. Sci. U. S. A.* **69**:3810–3814.
16. ROBBERSON, D. L., H. KASAMATSU, and J. VINOGRAD. 1972. Replication of mitochondrial DNA. Circular replicative intermediates in mouse L cells. *Proc. Natl. Acad. Sci. U. S. A.* **69**:737–741.
17. SEBRING, E. D., T. J. KELLY, JR., M. M. THOREN, and N. P. SALZMAN. 1971. Structure of replicating simian virus 40 deoxyribonucleic acid molecules. *J. Virol.* **8**:478–490.
18. TYLER, A. 1966. Incorporation of amino acids into protein by artificially activated non-nucleate fragments of sea urchin eggs. *Biol. Bull.* (*Woods Hole*). **130**:450–461.
19. TYLER, A., and B. TYLER. 1966. The gametes: some procedures and properties. *In* Physiology of Echinodermata. R. A. Boolootian, editor. Interscience Pubs., Inc., John Wiley & Sons, Inc., New York. 639–682.
20. VERHEY, C. A., and F. H. MOYER. 1967. Fine structural changes during sea urchin oogenesis. *J. Exp. Zool.* **164**:195–226.
21. VINOGRAD, J., J. LEBOWITZ, and R. WATSON. 1968. Early and late helix-coil transitions in closed circular DNA. The number of superhelical turns in polyoma DNA. *J. Mol. Biol.* **33**:173–197.
22. WOLSTENHOLME, D. R., K. KOIKE, and P. COCHRAN-FOUTS. 1973. Single strand-containing replicating molecules of circular mitochondrial DNA. *J. Cell Biol.* **56**:230–245.
23. WOLSTENHOLME, D. R., K. KOIKE, and P. COCHRAN-FOUTS. 1973. Replication of mitochondrial DNA: replicative forms of molecules from rat tissues and evidence for discontinuous replication. *Cold Spring Harbor Symp. Quant. Biol.* **38**:267–280.